Simulation of tectonic plates subduction with a multi-phase X–FEM model: level set representation, functional enrichment and numerical integration

Pedro Díez[1] and Sergio Zlotnik[2]

[1]Laboratori de Càlcul Numèric, Departament de Matemàtica Aplicada III, Universitat Politècnica de Catalunya Campus Nord UPC, 08034 Barcelona, Spain
[2]Group of Dynamics of the Lithosphere (GDL), Inst. of Earth Sci. "Jaume Almera", CSIC Lluís Solé i Sabarís s/n, 08028 Barcelona, Spain

ABSTRACT: the abstract

KEYWORDS: X-FEM, multiphase flow, plate tectonics, level sets

1 Introduction

A numerical model for plate tectonic subduction is presented. The subduction system behaves mechanically as a multiphase fluid governed by the Stokes equation. In the limit of creeping flow or the zero Reynolds number regime, the Stokes equation becomes a highly non-linear partial differential equation primarily because of non-linear constitutive relationship between the stress and strain-rate tensors. This mechanical problem is highly coupled with a thermal problem. The physical properties of the rocks (density, thermal conductivity, viscosity, etc.) are function of the temperature and pressure.

In this work the eXtended Finite Element Method (X-FEM) is used to numerically solve the problem. This includes a Level set technique to track the different phases and an enriched discretization using the partition of the unity approach.

In some simulations, the plate tectonics model requires accounting for more than two materials and thus standard X-FEM is not sufficient. Here, an extension of the level set technique and of the enriched interpolation are proposed, to track any number of free surfaces and improve the solution on the generated interfaces.

2 Problem statement

We model the subduction system as a n-phase incompressible fluid governed by the Stokes equation

$$\eta\nabla^2\mathbf{u} + \nabla p = \rho\mathbf{g} \qquad \text{in } \Omega \qquad (1a)$$

$$\nabla\cdot\mathbf{u} = 0 \qquad \text{in } \Omega \qquad (1b)$$

where η is the viscosity, ρ the density, $\mathbf{g}$ the acceleration due to gravity and p the pressure. The viscosity follows a creep power-law depending on the the composition, temperature, pressure and strain rate and thus it introduces a non-linear behavior to the mechanical problem. Due to geophysical timescale and viscosity, the intertial terms are neglected (Prandtl number = 10^{24}) and therefore equation (1a) is quasistatic, see [3] for further details.

The mechanical problem is coupled with a thermal problem

$$\rho C_p\left(\frac{\partial T}{\partial t} + \mathbf{u}\nabla T\right) = \nabla\cdot(k\nabla T) + \rho f \quad \text{in } \Omega \quad (2a)$$

where C_p is the isobaric heat capacity, k is the conductivity and f is the heat production term which depends on the strain rate.

3 Accounting for n-phases in a X-FEM framework

The location of the different phases is described by a collection of level set functions. The level sets represent material properties and they are consequently transported by the motion of the fluid. Thus the evolution of each one of the level sets, describing phase locations, is determined by pure advection equation

$$\dot{\phi}^{(i)} + \mathbf{u}\cdot\nabla\phi^{(i)} = 0 \qquad (3)$$

where $\mathbf{u}$ is the velocity field, solution of the Stoke's problem (1a), and $\phi^{(i)}$ is the level set number i.

3.1 Describing a n–phase fluid with $n-1$ level sets

One level set allows for describing only two phases (two subdomains). To include a third subdomain Ω_3 a second level set function $\phi^{(2)}$ is needed. We propose to assign a *hierarchy* to the level set functions: the subdomain Ω_1 is determined by the first level set $\phi^{(1)}$ as

$$\phi^{(1)}(\mathbf{x},t) = \begin{cases} > 0 & \text{for } \mathbf{x} \in \Omega_1 \\ \leq 0 & \text{for } \mathbf{x} \notin \Omega_1 \end{cases} \tag{4}$$

The curve where the level set $\phi^{(1)}(\mathbf{x},t)$ equals zero is the interface between the first phase and the rest of the domain. That is, either the second or the third phase. The remaining part in the simulation domain ($\mathbf{x} \in \Omega \backslash \Omega_1$) is split by the second level set $\phi^{(2)}$ as

$$\text{for } \mathbf{x} \notin \Omega_1,\ \phi^{(2)}(\mathbf{x},t) = \begin{cases} > 0 & \text{for } \mathbf{x} \in \Omega_2 \\ \leq 0 & \text{for } \mathbf{x} \in \Omega_3 \end{cases} \tag{5}$$

determining the location of the second and third sub domains. Note that the second level set does not have any influence where the first level set is positive. The first level set is "prior to" —or has upper hierarchy than— the second level set. Figure 3.1 shows the partition of the domain by two hierarchical level sets into three subdomains.

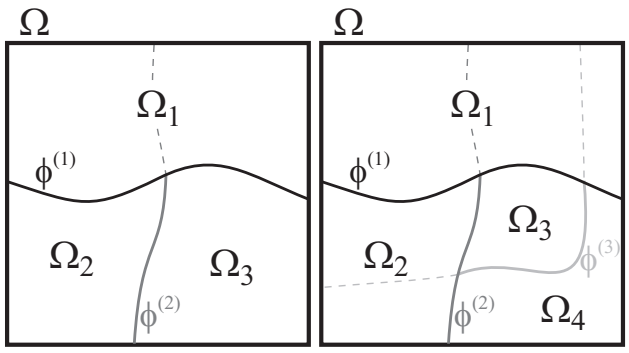

Figure 1: Two hierarchical level sets describe three material subdomains (left). In the right plot, three hierarchical level sets allows for describing four material phases.

This hierarchy phase description can be extended to the general case of n phases being tracked by $n-1$ level sets. In this case, the level sets describe the position of the phases by the following compact expression. The domain Ω_i expressed as a function of the the level sets $\{\phi^1, \phi^2, \ldots, \phi^{n-1}\}$ reads

$$\Omega_i = \text{supp}\big\{\langle\phi^i\rangle \prod_{j=1}^{i-1} \langle -\phi^j\rangle\big\}.$$

where we have made use of the McCauley brackets defined by

$$\langle\phi\rangle = 1/2\,(\phi + |\phi|).$$

4 X–FEM enrichment

The interface described by a level set does not need to conform with mesh edges, that leads to elements with different material properties in its interior. In X–FEM approach, the interpolation in those elements is enriched allowing the expected gradient discontinuity across the interface.

The interpolation of velocity $\mathbf{u}$ in enriched elements is composed by the standard finite element part, plus an enriched part. The second involves additional degrees of freedom $\mathbf{a}_j$ and its associated interpolation functions M_j

$$\mathbf{u}_h(\mathbf{x},t) = \sum_{j\in\mathcal{N}} \mathbf{u}_j(t)\, N_j(\mathbf{x}) + \sum_{j\in\mathcal{N}_{enr}} \mathbf{a}_j(t)\, M_j(\mathbf{x}) \tag{6}$$

where $\mathcal{N}$ is the set of standard finite element velocity degrees of freedom and $\mathcal{N}_{enr}$ is the set of enriched degrees of freedom. The $\mathcal{N}_{enr}$ set evolves trough time and needs to be recomputed at each time step after level set movement. The pressure field p is enriched in a similar way.

The interpolation function M_j is constructed as the product of standard nodal shape functions and a ridge function R

$$M_j(\mathbf{x}) = N_j(\mathbf{x}) R(\mathbf{x}). \tag{7}$$

The R function is based on the level set and has a "crest" just over the interface between materials. Several different ridge functions have been proposed in the literature (see for example [1, 2]). In the next sections a ridge function based on several hierarchical level sets is proposed. It is based on the ridge for two–phases used by Moës in [2].

4.1 Ridge function for two level sets

When two hierarchical level set are used two things have to be redefined. Firstly, the detection of enriched

element has to include the level set hierarchy. Secondly, the triple junction case, where two level sets intersects one element has to be considered.

The enriched element detection can be expressed as follows: find the elements crossed by $\phi^{(1)}$ and the elements crossed by $\phi^{(2)}$ with $\phi^{(1)}$ negative.

The ridge function R in enriched elements crossed by only the k–th level set is defined same as in previous case. The function $r^{(k)}$ is the ridge associated with level set k

$$r^{(k)} = \sum_{j \in \mathcal{N}_{enr}} |\phi_j^{(k)}| \, N_j - \left| \sum_{j \in \mathcal{N}_{enr}} \phi_j^{(k)} \, N_j \right| \tag{8}$$

where k is one or two for elements crossed by $\phi^{(1)}$ or $\phi^{(2)}$, respectively. The ridge function is $R = r^{(k)}$.

In the triple junction case, where two interfaces cross simultaneously one element, the ridge function has to take into account both level sets and the hierarchy between them. In this case R is defined as

$$R(\mathbf{x}) = r^{(1)}(\mathbf{x}) + r^{(2)}(\mathbf{x}) C^{(1)}(\mathbf{x}) \tag{9}$$

where the cutoff $C^{(1)}$ function introduces the level set hierarchy

$$C^{(1)}(\mathbf{x}) = \begin{cases} 1 & \text{if } \phi^{(1)}(\mathbf{x}) \leq 0 \\ r^{(1)}_{\text{norm}}(\mathbf{x}) & \text{otherwise} \end{cases} \tag{10}$$

Here $r^{(1)}_{\text{norm}}$ is the normalized ridge of the level set 1. The normalization process modifies the ridge leaving its crest with a constant value equal to one. Therefore, the cutoff function $C^{(1)}$ is continuous across the interface: $r^{(1)}_{\text{norm}}\big|_{interface} = 1$. The normalized ridge function, $r^{(1)}_{\text{norm}}$, is defined as

$$r^{(1)}_{\text{norm}} = \frac{\sum_{j \in \mathcal{N}_{enr}} |\phi_j^{(1)}| \, N_j - \left| \sum_{j \in \mathcal{N}_{enr}} \phi_j^{(1)} \, N_j \right|}{\sum_{j \in \mathcal{N}_{enr}} |\phi_j^{(1)}| \, N_j} \tag{11}$$

The cutoff $C^{(1)}$ function restricts the second ridge $r^{(2)}$ to the region where the first level set $\phi^{(1)}$ is negative, and smoothly reduces the value of $R^{(2)}$ where $\phi^{(1)}$ is positive. As the ridge function is constructed based on the level sets values it is modified through time. Despite the definition (11) does not include time explicitly, it inherits the time dependence of the level sets.

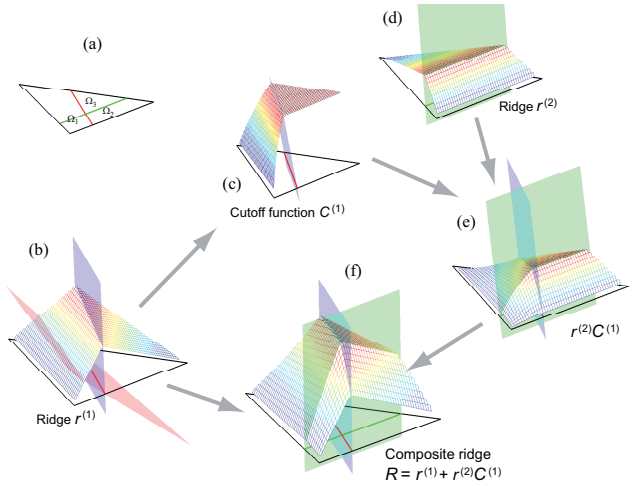

Figure 2: Construction of a composite ridge based in two hierarchical level sets. Plot (a) shows the element and the position of the interfaces. The ridge $r^{(1)}$ of the first level set $\phi^{(1)}$ is shown in (b). The cutoff function $C^(1)$ based on the first level set is shown in (c) The ridge $r^{(2)}$ of the second level set is shown in (d). Plot (e)shows the product $r^{(2)}C^(1)$. Finally, (f) is composite ridge.

The same idea is used to generalize the construction of the enrichment function to the case of more than two concurrent interfaces.

5 Numerical examples

The proposed n–phase approach is used to simulate some gravitational Raleigh–Taylor instabilities. Three fluid immiscible materials are modelled as different phases in Equation (1a). The driving force in all the presented models is the gravity; the lower buoyant layers are less dense than the overlying layers and a diapir develops.

The initial configuration of the following models is composed by three materials located as shown in figure 5. The upper layer is ten times denser than the two lower materials. As the lower materials have different viscosity the formed diapir looses its vertical axis of symmetry.

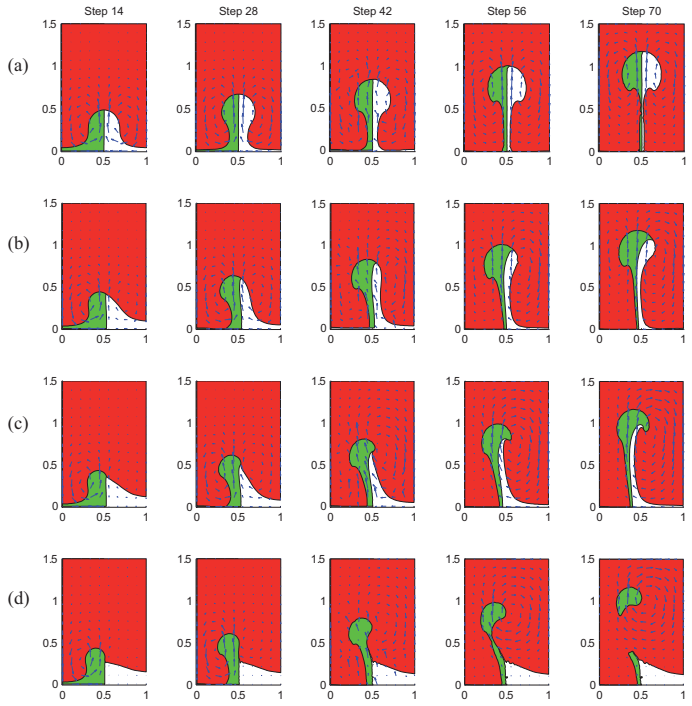

Figure 3: Several evolution of the 3–phase diapir. The difference of the four models (a), (b), (c) and (d) is the viscosity of the lower right material, which is 1, 5, 10 and 100, respectively. The other two materials have viscosity $\eta = 1$ in all models. The upper denser layer has a density of 10, while the two buoyant lower materials have a density of one.

The evolution of four models with different viscosity ratios between the two lower layers is shown in Figure 5. The (a) row corresponds to a model where all materials have the same viscosity $\eta = 1$. In this conditions the two buoyant materials behave as a unique fluid and a standard symmetric diapir develops. The second row in Figure 5 shows the evolution of the diapir when the viscosity of the right lower material (white) is five times larger than the viscosity of the other buoyant material (green). In this case the symmetry is lost. The evolution of the left half of the model is similar to the (a) row while the right half of the model is controlled by the viscosity contrast between the right material and the overburden layer. The models of the third and fourth rows have a viscosity contrast between the two lower layers of 10 and 100, respectively. The very viscous right material of the last model is almost stopped, while the left material develops the diapir alone. The generated flow change its main pattern during evolution. In the early stages (1st and 2nd snapshots) the high viscosity of the right material inhibits the movement in the right half and the flow is concentrated in the left part of the domain. This flux inclines the diapir to the left. Once the material gains enough height to loose the influence of the viscous layer (last two snapshots), the main flow moves to the right half of the model because there are more space facilitating the return flow. This right flux inclines the diapir to the right.

6 CONCLUSIONS

We have proposed and tested a methodology to extend the level set technique to track any number of free surfaces. The extension is based in a hierarchical ordering of several level set functions. To complete the X–FEM approach, the enrichment via partition of the unity method is also extended. The ridge function, base of the enriched interpolation, is restated to include several level sets and the hierarchy between them.

REFERENCES

[1] J. Chessa and T. Belytschko. An extended finite element method for two–phase fluids. *Transactions of the ASME*, pages 10–17, 2003.

[2] N. Moës, M. Cloirec, P. Cartaud, and J. F. Remacle. A computational approach to handle complex microstructure geometries. *Computer Methods in Applied Mechanics and Engineering*, 192:3163–3177, 2003.

[3] S. Zlotnik, P. Díez, M. Fernández, and J. Vergés. Numerical modelling of tectonic plates subduction using X–FEM. *Computer Methods in Applied Mechanics and Engineering*, 196:4283–4293, 2007.